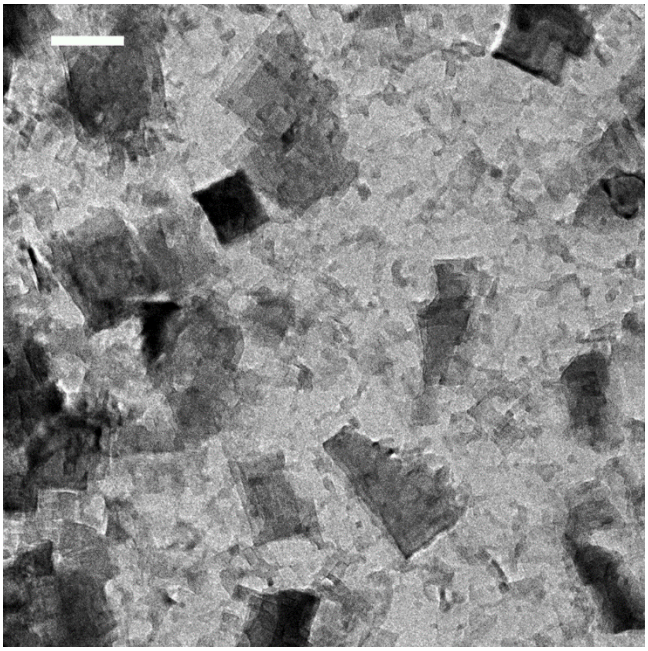

Supplementary Figure 1 | TEM of external salt byproducts. TEM image of some salt byproducts precipitated out separately from the Si network, with non-uniform particle size distribution. The scale bar is 50 nm.

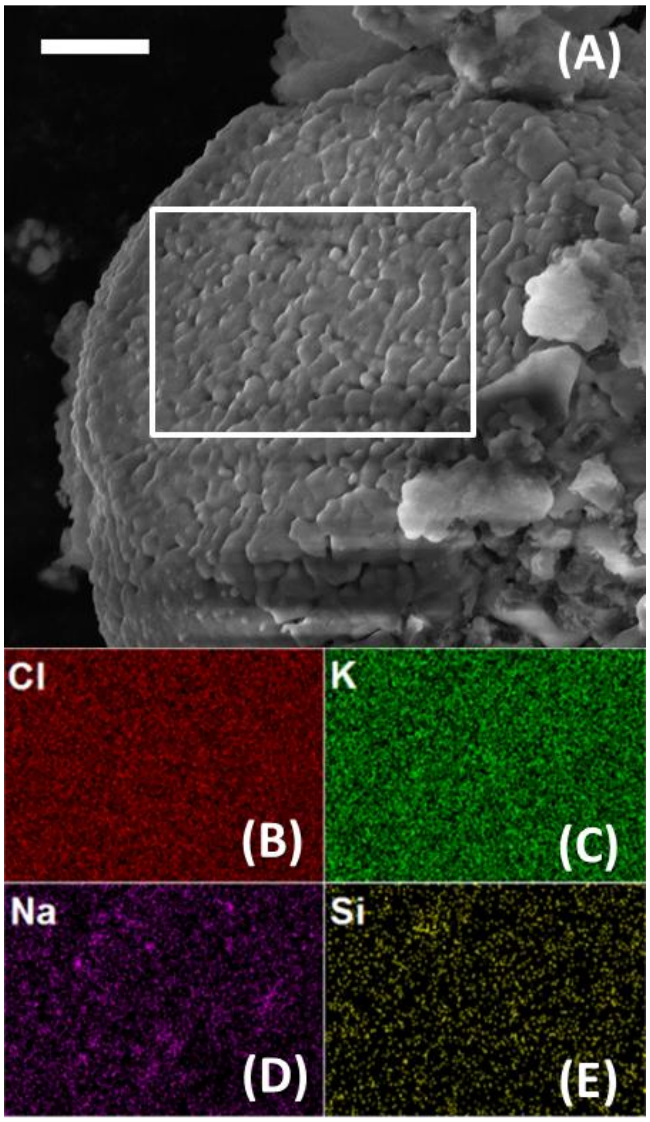

Supplementary Figure 2 | SEM and EDS of intermediate product. (A) Cross-section SEM image of intermediate product (scale bar is 5 μm), and EDS mapping of intermediate products – (B) Cl, (C) K, (D) Na, and (E) Si.

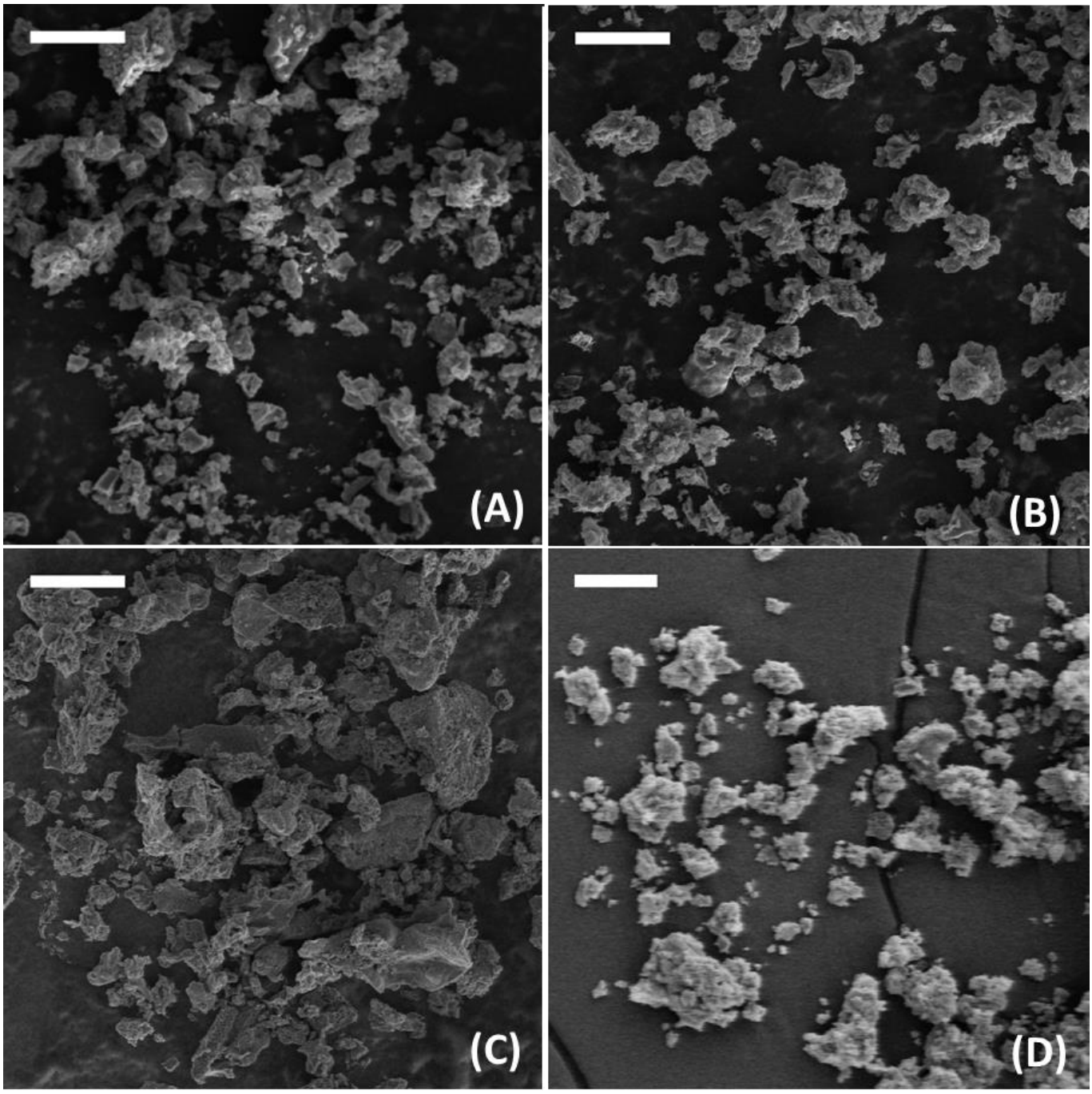
(A)
(B)
(C)
(D)

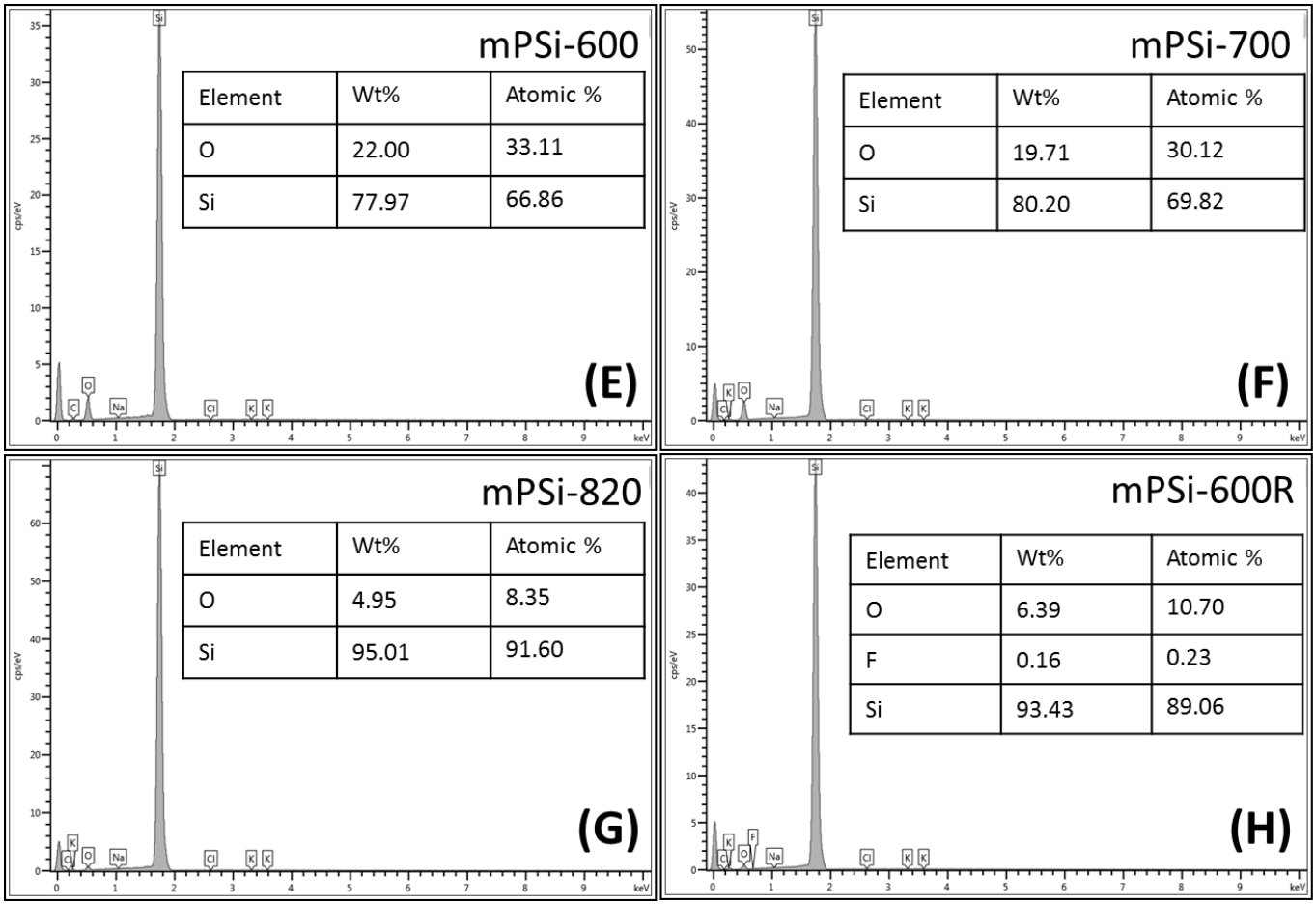

Supplementary Figure 3 | SEM images and EDS spectra of mPSi materials. SEM images of (A) mPSi-600; (B) mPSi-700; (C) mPSi-820 and (D) mPSi-600R. The scale bars are 20 µm. EDS spectra of (E) mPSi-600; (F) mPSi-700; (G) mPSi-820 and (H) mPSi-600R

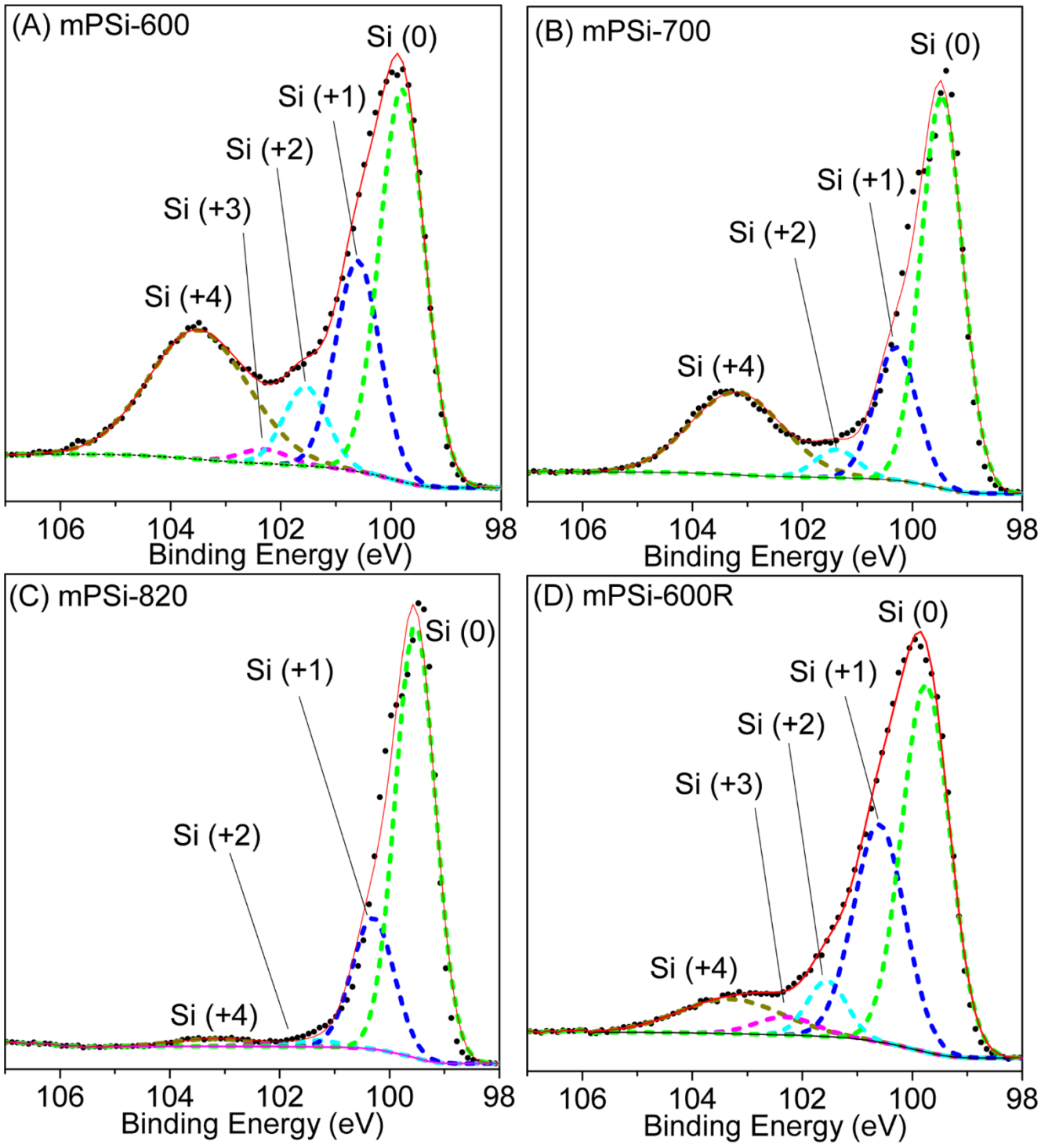

Supplementary Figure 4 | XPS fitting. The XPS spectra and their fitting results of (A) mPSi-600, (B) mPSi-700, (C) mPSi-820, (D) mPSi-600R.

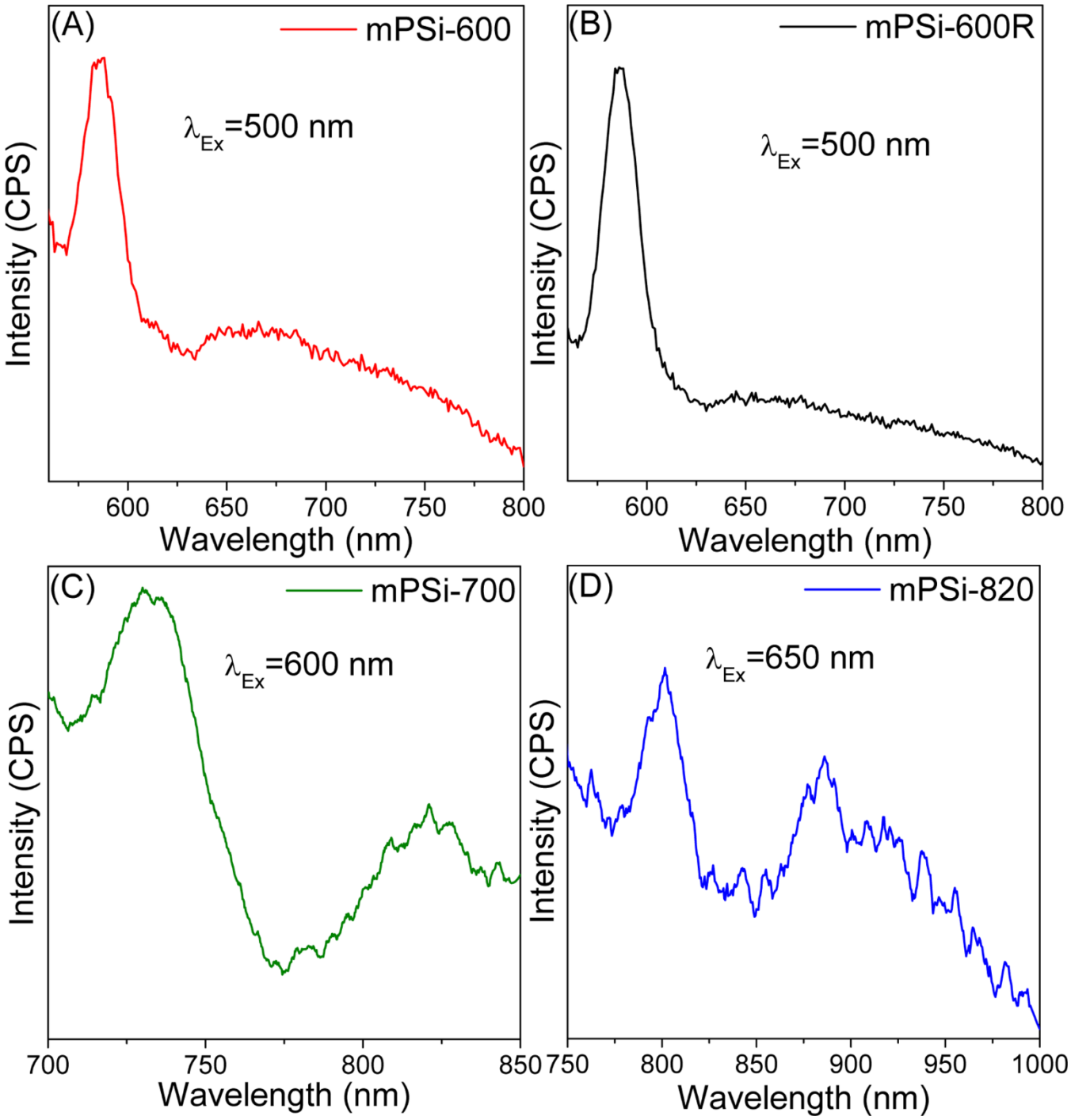

Supplementary Figure 5 | Photoluminescence spectra. Photoluminescence spectra of A) mPSi-600, B) mPSi-600R, C) mPSi-700, and D) mPSi-820.

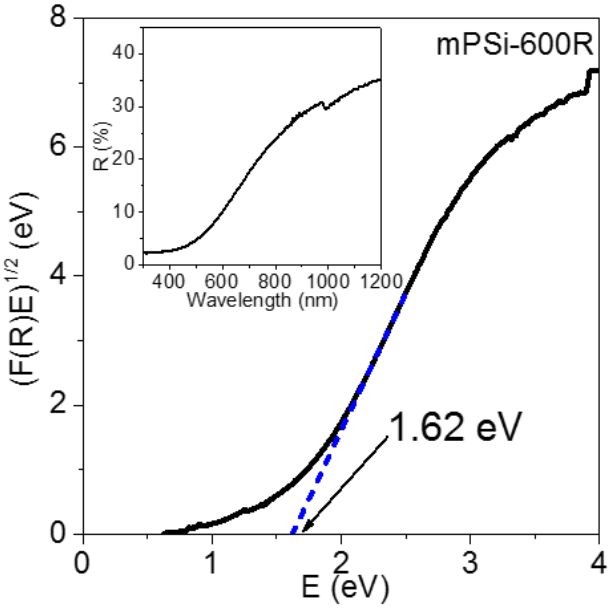

Supplementary Figure 6 | Optical spectra. Optical band gap and UV-Vis diffuse reflectance spectra (insert) of mPSi-600R.

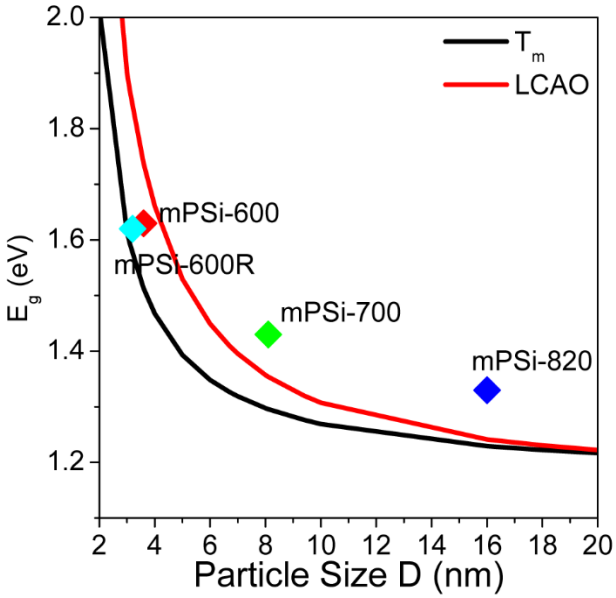

Supplementary Figure 7 | Measured and calculated band gaps. Optical band-gap energies for various Si crystallites with respect to their diameter D (nm). T_m and LCAO are corresponding to the theoretical relationship based on size-dependent temperature and linear combination of atomic orbitals technique.

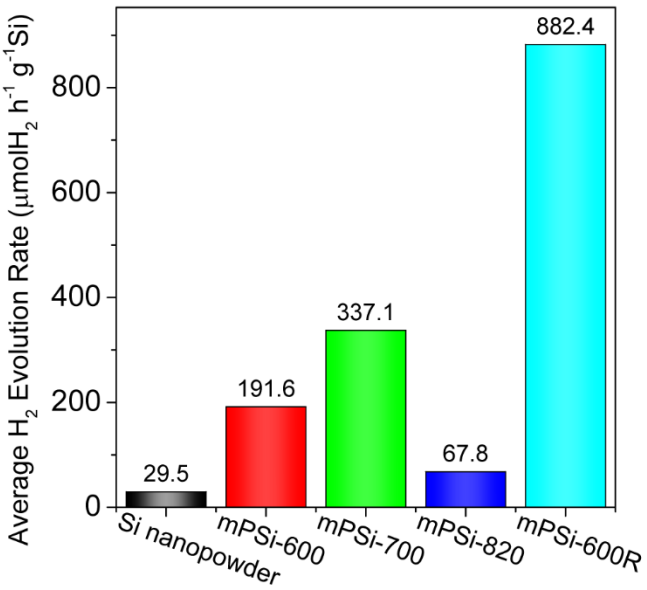

Supplementary Figure 8 | Average H_2 evolution. Average H_2 evolution rate of mPSi and Si nanopowder over 7 hours.

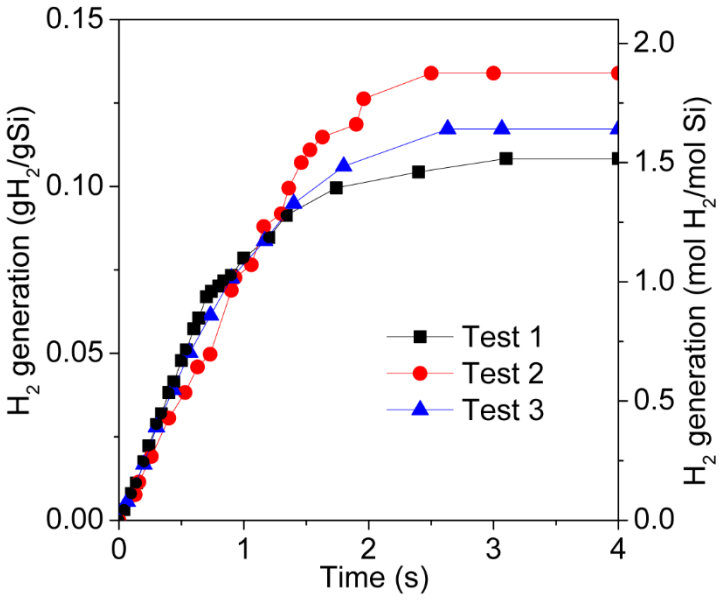

Supplementary Figure 9 | KOH reaction. Time course of H_2 generation by mPSi-600R chemically reacted with KOH aqueous solution.

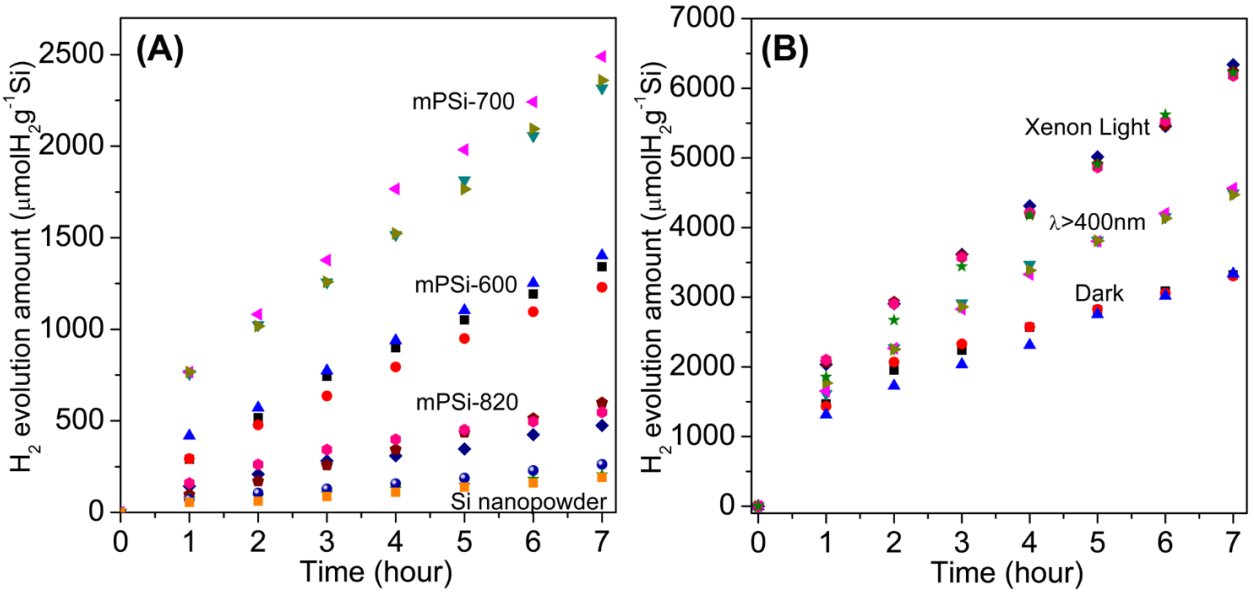

Supplementary Figure 10 | Repeatability of photocatalytic tests. (A) Typical reaction time course of the photocatalytic H_2 evolution of different porous Si materials without co-catalyst under 300 W Xenon light; (B) comparison of H_2 evolution activities of mPSi-600R under different light conditions.

Supplementary Table 1 | Oxygen concentration (at %) of all mPSi samples, determined from XPS.

Sample	O atomic ratio (atom %)
mPSi-600R	11.85
mPSi-600	32.15
mPSi-700	32.13
mPSi-820	8.65

Supplementary Table 2 | Primary Particle size, surface area, band gap, and H_2 evolution rate of mPSi materials and Si nano-powder.

	Primary Particle Size (nm)	BET surface area ($m^2 g^{-1}$)	Band gap (eV)	H_2 evolution rate ($\mu mol\ h^{-1}\ g^{-1}$Si in 7 hours)
Si nano-powder	≤50	70-100	1.40	29.5
mPSi-600	<10	497	1.65	191.6
mPSi-700	~10	321	1.43	337.1
mPSi-820	10-20	221	1.33	67.8
mPSi-600R	<10	580	1.62	882.4

Supplementary Discussion

Salt distribution in raw products

Some salt byproducts were found to precipitate out separately from the Si/salt matrixes, as shown in Supplementary Fig. 1. In a typical synthesis as described in the Method section, 9.95 g of salts were generated according to the stoichiometry of the reaction. The weight of the templating salts is at most 3.04 g (pore volume of 1.44 cm^3/g for mPSi-600). So, large amount of the salts precipitated out separately. In addition, extra reductant (1.2 fold to stoichiometric amount) was used in the synthesis to push the reaction to completion. After quenching the unreacted NaK by HCl/ether, an extra 1.99 g of salts should stoichiometrically have been generated. These salts also precipitated out separately. Without their growth being restricted by the silicon framework, we would expect these salts to grow larger than those within the framework. This is supported by TEM imaging; a representative image of these large salt particles is shown in Supplementary Fig. 1. It is clear that these external salts have a nonuniform particle size distribution from 10 nm to 50 nm, with individual particles being composed of smaller multi-crystals. The average crystallite size calculated from the XRD result (Fig. 2A) by the Scherrer equation is 22 nm for KCl and 31 nm for NaCl, which is still a reasonable number considering the multi-crystalline nature of those large salt particles.

Discussion of photoluminescence (PL) of all mPSi

Photoluminescence (PL) spectra of all the samples have been collected and shown in Supplementary Fig. 5. As the PL peak positions are related to the particle size and our particle size distribution is broader than in previous reports on the PL behavior of Si quantum dots, we can observe at least two peaks in the spectra. In comparison to the mPSi-600 and mPSi-600R samples, the PL peak intensity becomes lower and peak position shifts to a longer wavelength in the mPSi-700 and mPSi-820 samples, which matches the expected decrease in quantum confinement with increasing particle size. Both the PL phenomena and the shift of PL peaks prove the shift of band gap due to quantum confinement.[1]

Band gap-crystallite size relations

As shown in Supplementary Fig. 7, we have compared our experimentally-obtained band gap-crystallite size relationships with theoretical calculations based on a size-dependent temperature(T_m) model and linear combination of atomic orbitals (LCAO) technique.[2, 3] The crystallite sizes chosen for this calculation are based on applying the Scherrer equation to the XRD data for each sample. The band gap of mPSi-600 is in between the band gaps predicted by these two models, while the band gaps of mPSi-700 and mPSi-820 are slightly larger than the predicted values. The band gap from the UV-vis reflection measurements is the overall effect of the whole particle size distribution. As there are also some smaller particles in the mPSi-700 and mPSi-820 samples (as observed by HRTEM), and these smaller particles will contribute more than the larger ones to the observed band gap,[1] it is reasonable that our measured band gaps for these samples are slightly larger than the theoretical results. In addition, the amorphous Si and Si oxides present in the samples may also have some effect on the band gaps, but this effect is expected to be minor due to their low content.

Fitting of XPS peak components

We note that there is disagreement in the literature on the best way to fit SiO_x-containing XPS spectra. In addition, as demonstrated in a number of existing papers, it is important to have appropriate reference samples from which to get accurate peak parameters.[4-6] It is unclear what type of reference materials would accurately reflect the XPS peaks of our uniquely-structured mPSi materials, or how to fully account for factors such as variable oxide thickness effects or differential charging in our samples. Due to this lack of reliable reference samples and disagreement among existing publications on the best way to fit such spectra, the XPS peak fittings of our materials can only provide approximate fractions of oxide contents – they may not necessarily reflect the real composition distribution.

Supplementary References

1. Kux, A., Ben Chorin, M. Band gap of porous silicon. *Phys. Rev. B* **51**, 17535-17541 (1995).

2. Li, M., Li, J. C., Jiang, Q. Size-dependent band-gap and dielectric constant of Si nanocrystals. *Int. J. Mod Phys B* **24**, 2297-2301 (2010).

3. Delerue, C., Allan, G., Lannoo, M. Theoretical aspects of the luminescence of porous silicon. *Phys. Rev. B* **48**, 11024-11036 (1993).

4. Shallenberger, J. R. Determination of chemistry and microstructure in SiO_x ($0.1<x<0.8$) films by x-ray photoelectron spectroscopy. *J. Vac. Sci. Technol., A* **14**, 693-698 (1996).

5. Alexander, M. R., Short, R. D., Jones, F. R., Michaeli, W., Blomfield, C. J. A study of HMDSO/O_2 plasma deposits using a high-sensitivity and -energy resolution XPS instrument: curve fitting of the Si 2p core level. *Appl. Surf. Sci.* **137**, 179-183 (1999).

6. Iwata, S., Ishizaka, A. Electron spectroscopic analysis of the SiO_2/Si system and correlation with metal–oxide–semiconductor device characteristics. *J. Appl. Phys.* **79**, 6653-6713 (1996).